nature medicine

Heparin binding directs activation of T cells against adeno-associated virus serotype 2 capsid

Luk H Vandenberghe[1,2,4], Lili Wang[1,4], Suryanarayan Somanathan[1], Yan Zhi[1], Joanita Figueredo[1], Roberto Calcedo[1], Julio Sanmiguel[1], Ravi A Desai[3], Christopher S Chen[3], Julie Johnston[1], Rebecca L Grant[1], Guangping Gao[1] & James M Wilson[1]

Activation of T cells to the capsid of adeno-associated virus (AAV) serotype 2 vectors has been implicated in liver toxicity in a recent human gene therapy trial of hemophilia B[1]. To further investigate this kind of toxicity, we evaluated T-cell responses to AAV capsids after intramuscular injection of vectors into mice and nonhuman primates. High levels of T cells specific to capsids of vectors based on AAV2 and a phylogenetically related AAV variant were detected. Vectors from other AAV clades[2] such as AAV8 (ref. 3), however, did not lead to activation of capsid-specific T cells. Through the generation of AAV2-AAV8 hybrids and the creation of site-directed mutations, we mapped the domain that directs the activation of T cells to the RXXR motif on VP3, which was previously shown to confer binding of the virion to heparan sulfate proteoglycan (HSPG)[4–6]. Evaluation of natural and engineered AAV variants showed direct correlations between heparin binding, uptake into human dendritic cells (DCs) and activation of capsid-specific T cells. The role of heparin binding in the activation of CD8$^+$ T cells may be useful in modulating the immunogenicity of antigens and improving the safety profile of existing AAV vectors for gene therapy.

Skeletal muscle is considered a target for *in vivo* gene transfer of AAV vectors for applications of gene therapy and vaccines. Thus, we evaluated activation of T cells to the capsids of different AAV serotypes in mice and nonhuman primates after intramuscular injection.

We first cloned capsids from AAV2 and the recently identified serotypes AAV7 and AAV8 into adenoviruses and injected them intramuscularly into mice. This immunization approach assured effective delivery of capsid antigens into the classic endogenous major histocompatibility (MHC) class I pathway. Confirming previous findings[7], we detected high-level CD8$^+$ T cell responses and mapped the dominant epitopes in multiple strains of mice (data not shown). We next injected mice (C57Bl/6 and Balb/c) intramuscularly with 10^{11} genome-containing (GC) particles of AAV2, AAV7 and AAV8 and evaluated them for activation of T cells to capsid proteins by enzyme-linked ImmunoSPOT (ELISPOT; vectors contain the same genomes with AAV2 inverted terminal repeats encapsulated with capsids of different serotypes). We stimulated splenocytes with pooled peptides spanning the entire VP1 capsid as well as the mapped dominant peptides and analyzed T-cell responses (**Fig. 1**). AAV2 resulted in high T-cell frequencies against capsid; however, identical doses of AAV7 and AAV8 yielded very little evidence of T-cell activation against capsid despite the fact that *in vivo* transduction was at least five- to tenfold higher with AAV7 and AAV8 vectors as compared to AAV2 (**Table 1**). Serotype-specific differences in T-cell responses were independent of the strain of mice (**Fig. 1**), vector preparation or dose (data not shown).

We performed similar studies in cynomolgus macaques that received AAV vectors expressing HIV antigens (**Fig. 2**; for each serotype three vectors were pooled expressing gp140, RT and a gag-nef fusion). We injected macaques (five per group) intramuscularly with AAV2, AAV7 or AAV8, isolated peripheral blood mononuclear cells (PBMCs) from whole blood and assayed them for capsid-specific T cells using pooled VP1 peptides. Four of the five AAV2-injected macaques showed high T-cell frequencies against capsid; T cells from most of the AAV7- or AAV8-dosed macaques did not respond to capsid antigens (that is, T-cell frequency <2.5-fold higher than background). Notably, the T-cell responses to HIV-1 transgenes in these macaques did not reflect the qualitative or quantitative nature of the capsid T-cell responses in that robust transgene-specific T cells were measured, indicating an uncoupling of antigen processing and T-cell activation for capsids as compared to transgene product. The peak T-cell response to HIV-1 antigens as measured by interferon (IFN)-γ ELISPOT to gag, RT, nef and env for the three groups (mean $\pm$ s.d., $n = 5$ per group) was 855 ± 417 spot-forming units (SFU)/10^6 PBMCs for AAV2, 860 ± 190 for AAV7 and 774 ± 575 for AAV8.

Vectors made with AAV2-AAV8 hybrid capsids mapped a domain responsible for directing T cells to the capsid within the open reading frame for the gene encoding VP3 (data not shown). The VP3 protein comprises the structural backbone for the particle architecture as well as the majority of variable domains between AAV2 and AAV8

[1]Gene Therapy Program, Department of Pathology and Laboratory Medicine, University of Pennsylvania School of Medicine, 125 S. 31st Street, Philadelphia, Pennsylvania 19104, USA. [2]Molecular Medicine, Katholieke Universiteit Leuven, Kapucijnenvoer 33, B-3000 Leuven, Belgium. [3]Department of Bioengineering, University of Pennsylvania School of Engineering and Applied Science, 120 Hayden Hall, 3320 Smith Walk, Philadelphia, Pennsylvania 19104, USA. [4]These authors contributed equally to this work. Correspondence should be addressed to J.M.W. (wilsonjm@mail.med.upenn.edu).

Received 7 March; accepted 12 June; published online 16 July 2006; doi:10.1038/nm1445

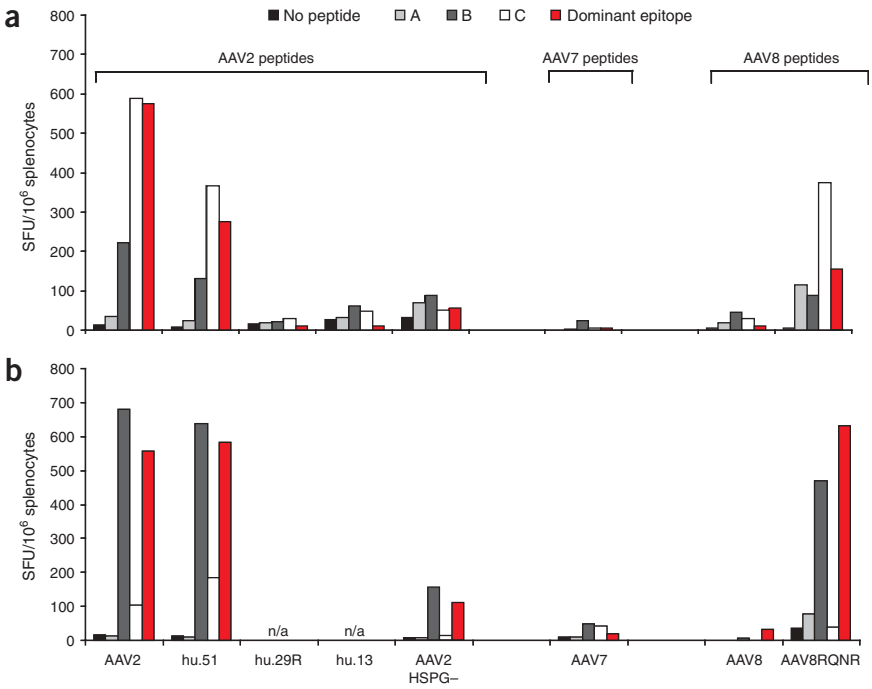

Figure 1 Activation of T cells in mice after administration of AAV. (**a**) Number of IFN-γ spot-forming units (SFU) in ELISPOT assay of splenocytes harvested 7 d after intramuscular injection of AAV in C57Bl/6. Several naturally occurring isolates of Clade B (AAV2, hu.51, hu.29R, hu.13) and mutants (AAV2HSPG–) were evaluated for T-cell responses. In addition, mice were injected with AAV8 and the AAV8 mutant RQNR to monitor T-cell activation. Cells were stimulated with three peptide pools (A, B and C) together spanning the entire AAV2 or AAV8 capsid, the C57Bl/6 dominant epitope for AAV2 or AAV8 or a 'no peptide' negative control. (**b**) Number of IFN-γ SFU in ELISPOT assay of splenocytes harvested 14 d after intramuscular injection of AAV in Balb/c mice. AAV2, hu.51 and the AAV2HSPG– mutant intramuscularly injected groups were stimulated with no peptide, comprehensive AAV2 peptide pools (A, B, C) and the AAV2 dominant epitope. Cells from AAV8- and AAV8RQNR-injected groups were incubated in the absence of peptide, with pooled AAV8 peptides or its dominant epitope peptide. In each case, the number of spots (*y* axis) is presented as a function of the injected vector (*x* axis) for different peptides (dominant and the pools) used to stimulate the cells. n/a, not assayed.

(refs. 8,9) that are thought to be responsible for their distinct biology. One of these regions on the AAV2 VP3 contains a heparin-binding domain characterized by a RXXR motif spanning residues 585 to 588 (refs. 5,6). To further study the potential role of heparin binding in directing the T-cell response to capsid, we studied vectors from other members of the Clade B family to which AAV2 belongs, including one that retains the RXXR motif (that is, hu.51) and two that do not (that is, hu.29R and hu.13; **Table 1**). The presence of an intact heparin-binding motif correlated with capsid T-cell responses (**Fig. 1**); hu.13 differs from AAV2 at only two residues other than in the heparin-binding domain, which suggests that this domain is important. Transgene expression from the heparin binding–deficient Clade B variants was indistinguishable from that seen with the heparin-binding variants in terms of expression of the reporter gene encoding α1-antitrypsin (A1AT) after muscle-directed gene transfer (**Table 1**). Definitive confirmation of the role of the RXXR motif in directing the capsid T-cell response was provided in two engineering experiments. First, we ablated the heparin-binding site in AAV2 by converting RGNR to SGNT, which is the consensus sequence from analysis of 15 Clade B, non–heparin-binding AAV isolates (**Table 1**); the resulting vector did not activate T cells to capsid (**Fig. 1**). Second, we converted the corresponding residues in AAV8 to a motif that should confer binding to heparin (that is, QQNT to RQNR; **Table 1**); the AAV8 variant with the reconstructed heparin binding site activated high levels of capsid-reactive T cells (**Fig. 1**). The presence or absence of heparin binding on AAV capsid did not seem to influence the type of T helper responses (that is, T_H1 or T_H2) as measured by capsid IgG isotypes and antigen-stimulated secretion of cytokines from splenocytes (data not shown).

Table 1 Description of AAV isolates and mutants

AAV isolate or mutant	AAV clade	RXXR domain	Distance from AAV2 outside RXXR	Heparin column binding	Vector production (GC)	Gene transfer efficiency (μg/ml) Muscle	Gene transfer efficiency (μg/ml) Liver
AAV2	B	RGNR	0/738	+	$1.8 \pm 0.8 \times 10^{13}$	3.1 ± 0.3	4.9 ± 1.5
hu.51	B	RGNR	4/738 *(G133, G423, T447, N529)*	+	$6.8 \pm 3.9 \times 10^{12}$	2.3 ± 0.5	1.9 ± 0.4
AAV8RQNR	E	RQNR	119/738	+	$1.1 \pm 0.2 \times 10^{12}$	n/a	n/a
hu.29R	B	SGNT	5/738 *(A151, S162, N164,S179, P547)*	–	$3.7 \pm 1.5 \times 10^{13}$	2.7 ± 0.5	1.8 ± 0.5
hu.13	B	GGNT	2/738 *(A151, S205)*	–	$2.9 \pm 1.5 \times 10^{13}$	1.8 ± 0.4	1.6 ± 0.5
AAV2HSPG–	B	SGNT	0/738	–	$1.0 \pm 0.5 \times 10^{13}$	n/a	n/a
AAV8	E	QQNT	119/738	–	$3.2 \pm 1.7 \times 10^{13}$	38.0 ± 9.3	60.1 ± 4.3
AAV7	D	AANT	127/738	n/a	$3.2 \pm 2.1 \times 10^{13}$	13.4 ± 3.5	60.1 ± 12.6

Name of the isolate or mutant, its phylogenetic clade, amino acid sequence at AAV2-parallel RXXR motif, heparin column binding affinity (+: specific binding, –: no binding) and the distance from AAV2 outside of RXXR domain is provided. The distance is given in number of different residues outside of RXXR when compared to AAV2. For Clade B members, amino acid differences are presented with their coordinates. In addition, average yield from a minimum of three vector preparations is given with standard deviation. Gene-transfer efficiency in C57Bl/6 ($n = 5$) mice is represented by average and standard deviation of A1AT serum levels after gene delivery with the respective capsid isolate 28 d after intramuscular injection (muscle) and after intraportal injection (liver). n/a, not assayed.

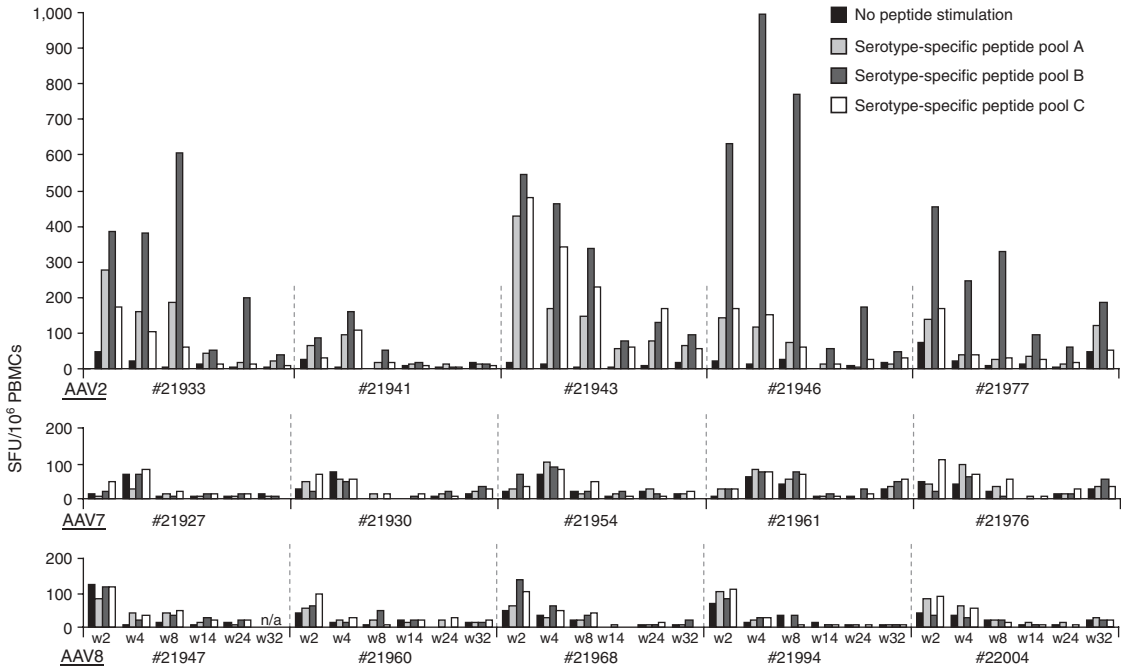

Figure 2 Time course of T-cell response to AAV capsid in cynomolgus macaques after intramuscular vaccinations with AAV vectors of different serotypes. Monkeys were immunized by intramuscular injection of a mixture of 10^{12} GC each of AAV.CMV.HIVgp140, AAV.CMV.HIVGN2 and AAV.CMV.HIV RT3. At weeks 2, 4, 8, 14, 24 and 32 after immunization, IFN-γ ELISPOT assay was performed on PBMCs. A total of 15 macaques were dosed, with five macaques per vector serotype (top, AAV2; center, AAV7; bottom, AAV8). The frequency of spots as measured by ELISPOT is presented as a function of time, noted in weeks (for example, w8) for the individual macaques, which are identified by five-digit numbers. For each assay, three peptide pools (A, B and C) spanning the entire VP1 region of the corresponding capsids were used. n/a, not assayed.

A subset of the natural and engineered AAV variants was further evaluated for biochemical and cellular evidence of binding to heparin. Purified preparations of vectors were passed over a heparin-binding column and the flow-through was analyzed for vector genomes. We observed virtually complete binding of the RXXR-containing variants (AAV2, hu.51 and AAV8RQNR), whereas we found substantial quantities of vector in the flow-through for vectors lacking the RXXR motif (hu.29R, hu.13, AAV2HSPG– and AAV8; **Table 1**). We also evaluated vectors for binding to HeLa and CHO cells by incubation at 4 °C and subsequent analysis of washed cells for retention of vector genomes. **Figure 3a** shows binding relative to that observed with AAV2. Binding of AAV8 and the AAV2 variant with the ablated heparin-binding site (AAV2HSPG–) was substantially reduced for both cell lines, as was binding of AAV2 in the presence of heparin. Reconstruction of the RXXR motif in AAV8 confers cell binding to levels in excess of that seen with AAV2.

The emerging hypothesis is that HSPG-mediated uptake of vector by DCs is a rate-limiting step in the activation of T cells against capsid. We examined this *in vitro* using primary cultures of human monocyte–derived DCs. Binding studies showed identical results to those observed with the cell lines (**Fig. 3a**); all RXXR-containing vectors bound DCs, whereas those without this domain did not bind as well. Binding of AAV to DCs was visualized directly by microscopy using fluorescently labeled AAV2 together with indirect immunofluorescence with an antibody to HSPG (**Fig. 3b**). AAV2 bound to the surface of the cells in discrete foci that colocalized with HSPG. No detectable binding of AAV2 was observed in the presence of excess heparin (data not shown).

The importance of these findings to gene therapy stems, in part, from a study in which the authors ascribed dose-limiting toxicity in a hemophilia B clinical trial to cytolytic T cells directed against hepatocytes presenting AAV2 capsid epitopes[1]. They also suggested that this problem will not be overcome through the use of alternative serotypes, as the T-cell epitopes are likely to be conserved. Our studies indicate that the critical path to activation of T cells to capsid is not a function of MHC class I restriction, but rather is dependent on the binding of capsid to HSPG. We show in both mice and nonhuman primates that non–heparin-binding engineered or natural variants of AAV are less likely to activate T cells to the capsid. All members of AAVs from Clades A, C, D, E and F are missing the RXXR motif, and those that have been studied do not bind heparin with the avidity of AAV2 (ref. 10); this includes AAV8 and AAV9, which show superior transduction profiles to liver and heart, respectively. In fact, some members of the Clade B family such as hu.13 (ref. 2), which are virtually identical to AAV2 except in the heparin-binding domain, retain levels of *in vivo* gene transfer similar to AAV2 without the problem of capsid T cells (**Table 1** and **Fig. 1**).

The mechanism by which heparin binding directs the activation of T cells to the capsid is unclear. HSPG has been shown to bind to DCs and promote their activation[11,12]. We speculate that binding of capsid to HSPG shuttles the virion into a DC pathway that leads to its processing and MHC class I presentation. Pathways by which this occurs begin with endocytotic or phagocytotic uptake followed by a series of proteolytic steps and eventual loading of peptides onto MHC class I complexes[13]. It is unclear where along these pathways HSPG binding promotes the process of cross-presentation. It is interesting that these pathways are independent of vector transduction, as heparin binding–deficient virions of various clades retain excellent transduction profiles. Furthermore, heparin binding is not necessary for T-cell responses to the transgene; we observed high-level T-cell responses to

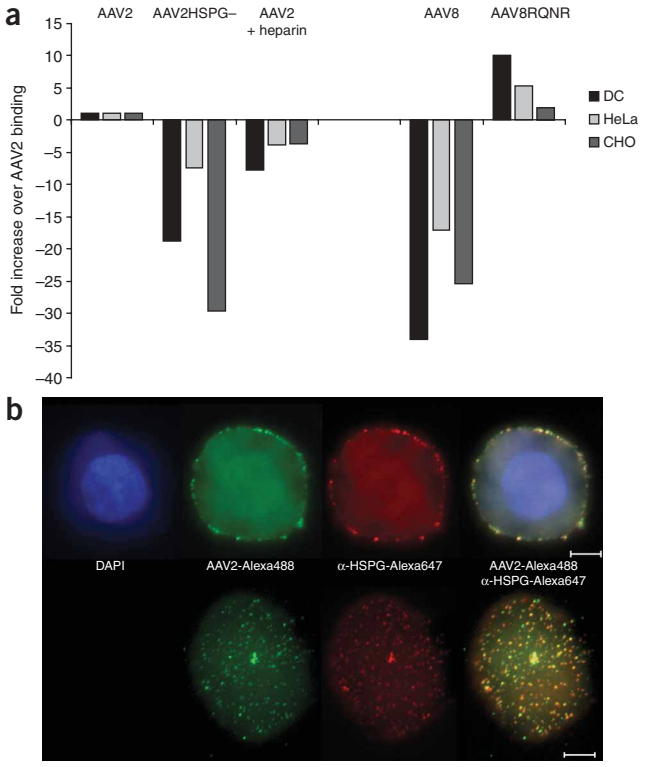

Figure 3 Impact of HSPG affinity on AAV binding. (**a**) Relative binding of AAVs to human monocyte-derived DCs, HeLa and CHO cells when compared to AAV2. Cell binding was evaluated for AAV2, AAV2HSPG–, AAV2 in the presence of heparin, AAV8 and AAV8RQNR. DNase-resistant genome copies were measured by quantitative PCR. The values relative to those from the AAV2-bound virus condition are presented as fold increase; a positive number represents binding greater than AAV2 and a negative number represents binding less than AAV2. (**b**) Colocalization of AAV2 and cell-surface heparan sulfate proteoglycan (HSPG) on primary human DCs. AAV2-Alexa488 (green) and antibody against HSPG conjugated with Alexa647 (red) on the cell surface of primary human DCs is visualized. Foci of colocalized HSPG and AAV2 are yellow on the overlaid image (right). Representative DCs are visualized with a 63× objective in two different focal planes representing a cross-section of the cell (top) and the cell surface (bottom). Nuclear DAPI staining of the cross-section is shown in blue. Scale bar, 5 μm.

transgene products from the non–heparin binders, AAV7 and AAV8, which remains a potential safety issue for the treatment of genetic deficiency states. Finally, AAV presents an interesting divergence of MHC class I pathways directed by the structure of its capsid.

METHODS

Vectors. All natural isolates have been previously described[2,3,9]. AAV2HSPG– and AAV8RQNR were generated by R585S, R588T and Q588R, T591R mutagenesis, respectively (Quickchange II, Stratagene). hu.29R was optimized for better production after a G396E change. The junctions between AAV2-AAV8 hybrids were engineered either at the VP2 start position or in a conserved region proximal to the VP3 start codon (660 bp past the VP1 start). We generated packaging constructs and performed vector production as previously described[3]. The AAV2 vector lots used were either CsCl or heparin column purified. We performed the mouse immunization studies both with a nuclear targeted *lacZ* or an hA1AT transgene driven from an enhanced chicken β-actin promoter. We used the following vectors in primate studies: AAV.CMV.HIVgp140, AAV.CMV.HIVRT3 and AAV.CMV.HIVGN2; vectors were packaged with AAV2, AAV7 or AAV8 serotypes.

Cells and binding studies. We maintained adherent cultures of HeLa and CHO cells according to ATCC and released cells nonenzymatically after incubation with cell dissociation solution (Sigma-Aldrich). We cultured human primary DCs from PBMCs provided by the Center for AIDS Research at the University of Pennsylvania. Briefly, we cultured plastic adherent monocytes for 7 d in the presence of granulocyte-macrophage colony-stimulating factor (GM-CSF; Berlex) and interleukin (IL)-4 (R&D). We phenotyped immature DCs using the following markers: CD11c, CD80, CD86, CD83, HLA-DR, CD14 and DC-SIGN (BD Biosciences). Viral binding was preceded by 30 min incubation on ice of 10^{10} particles in the presence of 20 units of heparin salt (Sigma-Aldrich) or an equal volume PBS. We incubated cells (10^6) on a rocking platform at 4 °C for 3 h, recovered them by centrifugation and washed them three times with serum-free AIM-V culture medium (Invitrogen). The supernatant obtained after resuspension in a 400 mM NaCl solution and three freeze-thaw cycles was assayed for AAV genomes by Taqman PCR. We performed heparin column binding experiments with HiTrap Heparin HP columns (Amersham Biosciences).

Animal studies. Male C57Bl/6 and Balb/c were obtained from Charles River Laboratories. We administered 10^{11} GC by intramuscular injection to mice in the hind limb at two injection sites. Cynomolgus macaques were treated and cared for at Barton's West End Facilities in Oxford, New Jersey. Blood samples were taken by venipuncture of the saphenous vein. We isolated PBMCs as previously described[14]. Each primate received intramuscular injections of a mixture of three AAV vectors carrying different HIV antigens (gp140, RT and gag-nef fusion). We injected five macaques with 10^{12} particles per vector for the AAV2, AAV7 and AAV8 group. We injected the vector mixture in a total volume of 1 ml PBS at two sites into the right quadriceps femoris with a 25-gauge needle. Experimental protocols were approved by the Institutional Animal Care and Use Committee of the University of Pennsylvania, and use of the vectors in the protocols was approved by the Environmental Health and Radiation Safety Office and the Institutional Biosafety Committees of the University of Pennsylvania.

Immunologic assays. We performed IFN-γ ELISPOT assays using previously described protocols for monkeys[15] and mice[16,17]. Peptide libraries derived from the VP1 of AAV2, AAV7 or AAV8 proteins were synthesized as 15-mers with 10–amino acid overlap with the preceding peptide (Mimotopes) and dissolved in DMSO at approximately 100 mg/ml. For AAV T-cell assays, the peptide library for each serotype was divided into three pools such that pool 2A contained the first 50 peptides of AAV2 VP1, pool 2B contained peptides 51–100 and pool 2C contained peptides 101–145. Peptides corresponding to dominant epitopes were obtained from Invitrogen or Mimotopes and solubilized in DMSO (4 mg/ml). Dominant H-2^b–restricted epitopes SNYNKSVNV (AAV2), NSLVNPGVA (AAV7) an NSLANPGIA (AAV8) were used in the C57Bl/6 mice. Experiments with Balb/c mice were done with the following H-2^d–restricted epitopes: VPQYGYLTL (AAV2) and IPQYGYLTL (AAV7 and AAV8). Peptides were used at the concentration of 2 μg/ml in all experiments; DMSO concentrations were kept below 0.1% (vol/vol) in all final assay mixtures. Spots were counted with an ELISPOT reader (AID). In addition to peptide stimulation, we performed a 'no peptide' condition and nonspecific stimulation with staphylococcal enterotoxin B (SEB) and phorbol 12-myristate 13-acetate (PMA)/ionomycin controls. Spot numbers were normalized for cell numbers with the PMA/ionomycin values in order to account for slight variation in cell density in the ELISPOT assay. We performed cytokine release assays on splenocytes of mice immunized with either AAV2 or AAV2HSPG–. We stimulated cells with the AAV2 VP1 peptide pools and assayed supernatant for IL-4, IL-10, IFN-γ and IL-2. We monitored IgG isotype responses by ELISA and established relative levels through limiting dilution.

Microscopy. We conjugated AAV2 and the F58-10E4 antibody against HSPG (Seikagaku) with Alexa Fluor 488 and Alexa Fluor 647 Protein Labeling Kit (Invitrogen). We incubated cells at 4 °C for 1 h with virus and antibody in the presence or absence of heparin and subsequently washed them three times in a mixture of PBS, 2.5% FBS and 0.1% NaN3 before mounting them on slides. Microscopy was performed with an inverted Zeiss Axiovert 200M (Carl Zeiss MicroImaging).

ACKNOWLEDGMENTS

We would like to acknowledge J. Franco and the support of Z. Abbas, Y. Li, E. McComb, R. Patel, A. Wang and E. Wolf from the Vector Core of the University of Pennsylvania. R. Desai is supported by a graduate research fellowship from the National Science Foundation. Microscopy equipment was financed with grants from the National Heart, Lung, and Blood Institute (HL073305) and National Institute of Biomedical Imaging and BioEngineering (EB00262). The research was funded by grants from GlaxoSmithKline and the US National Institutes of Health (P01-HL-059407 and P30-DK-047757).

COMPETING INTERESTS STATEMENT

The authors declare competing financial interests (see the *Nature Medicine* website for details).

Published online at http://www.nature.com/naturemedicine/
Reprints and permissions information is available online at http://npg.nature.com/reprintsandpermissions/

1. Manno, C.S. *et al.* Successful transduction of liver in hemophilia by AAV-Factor IX and limitations imposed by the host immune response. *Nat. Med.* **12**, 342–347 (2006).
2. Gao, G. *et al.* Clades of Adeno-associated viruses are widely disseminated in human tissues. *J. Virol.* **78**, 6381–6388 (2004).
3. Gao, G.P. *et al.* Novel adeno-associated viruses from rhesus monkeys as vectors for human gene therapy. *Proc. Natl. Acad. Sci. USA* **99**, 11854–11859 (2002).
4. Summerford, C. & Samulski, R.J. Membrane-associated heparan sulfate proteoglycan is a receptor for adeno-associated virus type 2 virions. *J. Virol.* **72**, 1438–1445 (1998).
5. Kern, A. *et al.* Identification of a heparin-binding motif on adeno-associated virus type 2 capsids. *J. Virol.* **77**, 11072–11081 (2003).
6. Opie, S.R., Warrington, K.H., Jr., Agbandje-McKenna, M., Zolotukhin, S. & Muzyczka, N. Identification of amino acid residues in the capsid proteins of adeno-associated virus type 2 that contribute to heparan sulfate proteoglycan binding. *J. Virol.* **77**, 6995–7006 (2003).
7. Sabatino, D.E. *et al.* Identification of mouse AAV capsid-specific $CD8^+$ T cell epitopes. *Mol. Ther.* **12**, 1023–1033 (2005).
8. Xie, Q. *et al.* The atomic structure of adeno-associated virus (AAV-2), a vector for human gene therapy. *Proc. Natl. Acad. Sci. USA* **99**, 10405–10410 (2002).
9. Gao, G. *et al.* Adeno-associated viruses undergo substantial evolution in primates during natural infections. *Proc. Natl. Acad. Sci. USA* **100**, 6081–6086 (2003).
10. Halbert, C.L., Allen, J.M. & Miller, A.D. Adeno-associated virus type 6 (AAV6) vectors mediate efficient transduction of airway epithelial cells in mouse lungs compared to that of AAV2 vectors. *J. Virol.* **75**, 6615–6624 (2001).
11. Kodaira, Y., Nair, S.K., Wrenshall, L.E., Gilboa, E. & Platt, J.L. Phenotypic and functional maturation of dendritic cells mediated by heparan sulfate. *J. Immunol.* **165**, 1599–1604 (2000).
12. Shikano, S., Bonkobara, M., Zukas, P.K. & Ariizumi, K. Molecular cloning of a dendritic cell-associated transmembrane protein, DC-HIL, that promotes RGD-dependent adhesion of endothelial cells through recognition of heparan sulfate proteoglycans. *J. Biol. Chem.* **276**, 8125–8134 (2001).
13. Wilson, N.S. & Villadangos, J.A. Regulation of antigen presentation and cross-presentation in the dendritic cell network: facts, hypothesis, and immunological implications. *Adv. Immunol.* **86**, 241–305 (2005).
14. Mueller, Y.M. *et al.* Interleukin-15 increases effector memory $CD8^+$ T cells and NK cells in simian immunodeficiency virus-infected macaques. *J. Virol.* **79**, 4877–4885 (2005).
15. Reyes-Sandoval, A. *et al.* Human immunodeficiency virus type 1-specific immune responses in primates upon sequential immunization with adenoviral vaccine carriers of human and simian serotypes. *J. Virol.* **78**, 7392–7399 (2004).
16. Simmons, G. *et al.* Identification of murine T-cell epitopes in Ebola virus nucleoprotein. *Virology* **318**, 224–230 (2004).
17. Zhi, Y. *et al.* Identification of murine CD8 T cell epitopes in codon-optimized SARS-associated coronavirus spike protein. *Virology* **335**, 34–45 (2005).